Article

Cell Reports

Evasion of Cell Senescence Leads to Medulloblastoma Progression

Graphical Abstract

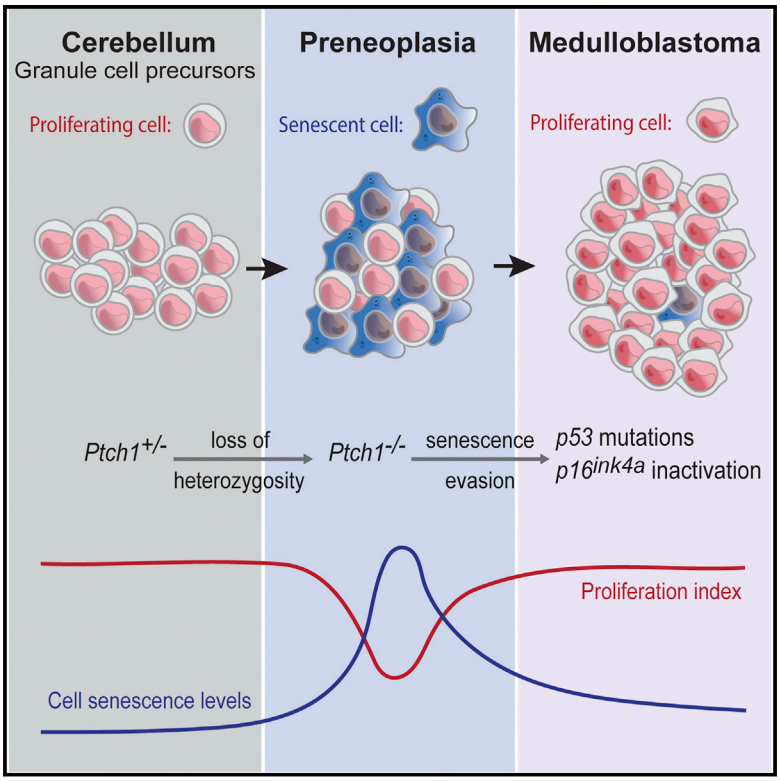

Authors

Lukas Tamayo-Orrego, Chia-Lun Wu, Nicolas Bouchard, ..., Patryk Skowron, Michael D. Taylor, Frédéric Charron

Correspondence

frederic.charron@ircm.qc.ca

In Brief

How brain tumors develop from precancerous lesions is not well understood. Using *Ptch1* heterozygous mice, Tamayo-Orrego et al. show that medulloblastoma preneoplastic lesions display *Ptch1* loss of heterozygosity and cell senescence, a tumor-suppressive mechanism. Subsequently, spontaneous *p53* mutations or *p16ink4a* inactivation leads to senescence evasion and medulloblastoma progression.

Highlights

- Medulloblastoma preneoplastic lesions exhibit *Ptch1* loss of heterozygosity
- Medulloblastoma preneoplasia display high levels of cell senescence
- Spontaneous *p53* mutations or *p16ink4a* inactivation leads to senescence evasion
- Cell senescence is a tumor-suppressive mechanism for medulloblastoma

Tamayo-Orrego et al., 2016, Cell Reports *14*, 2925–2937
March 29, 2016 ©2016 The Authors
http://dx.doi.org/10.1016/j.celrep.2016.02.061

Cell Reports
Article

Evasion of Cell Senescence Leads to Medulloblastoma Progression

Lukas Tamayo-Orrego,[1,2] Chia-Lun Wu,[1,3] Nicolas Bouchard,[1,3] Ahmed Khedher,[1] Shannon M. Swikert,[1,2] Marc Remke,[4] Patryk Skowron,[5] Michael D. Taylor,[5] and Frédéric Charron[1,2,3,6,*]

[1]Molecular Biology of Neural Development, Institut de Recherches Cliniques de Montréal, 110 Pine Avenue West, Montreal, QC H2W 1R7, Canada
[2]Integrated Program in Neuroscience, McGill University, Montreal, QC H3A 2K6, Canada
[3]Department of Medicine, University of Montreal, Montreal, QC H3T 1J4, Canada
[4]Research Group "Non-coding RNAs in Pediatric Cancers," German Cancer Consortium, University Hospital Düsseldorf, Department of Pediatric Oncology, Hematology, and Clinical Immunology, 40225 Düsseldorf, Germany
[5]Division of Neurosurgery and The Arthur and Sonia Labatt Brain Tumour Research Centre, Hospital for Sick Children, 555 University Avenue, Toronto, ON M5G 1X8, Canada
[6]Division of Experimental Medicine, Department of Medicine, Department of Anatomy and Cell Biology, Department of Biology, McGill University, Montreal, QC H3A 2B2, Canada
*Correspondence: frederic.charron@ircm.qc.ca
http://dx.doi.org/10.1016/j.celrep.2016.02.061

SUMMARY

How brain tumors progress from precancerous lesions to advanced cancers is not well understood. Using *Ptch1*$^{+/-}$ mice to study medulloblastoma progression, we found that *Ptch1* loss of heterozygosity (LOH) is an early event that is associated with high levels of cell senescence in preneoplasia. In contrast, advanced tumors have evaded senescence. Remarkably, we discovered that the majority of advanced medulloblastomas display either spontaneous, somatic *p53* mutations or *Cdkn2a* locus inactivation. Consistent with senescence evasion, these *p53* mutations are always subsequent to *Ptch1* LOH. Introduction of a *p53* mutation prevents senescence, accelerates tumor formation, and increases medulloblastoma incidence. Altogether, our results show that evasion of senescence associated with *Ptch1* LOH allows progression to advanced tumors.

INTRODUCTION

For a certain number of human malignancies, it has been possible to examine different stages of tumor progression and correlate different histopathological stages with specific genetic events (Fearon and Vogelstein, 1990). More recently, an emerging paradigm proposes that oncogenic changes associated with the formation of precancerous lesions lead to cell senescence, a mechanism that restrains tumor progression in vivo (Braig et al., 2005; Chen et al., 2005; Michaloglou et al., 2005). Brain tumors constitute a challenge for investigating tumor progression because precancerous lesions are rarely detected. Medulloblastoma is the most common brain tumor in children, and deregulation of hedgehog signaling characterizes 25% of human medulloblastomas (Taylor et al., 2012). Although genomic studies have revealed recurrent genetic and epigenetic alterations in human sonic hedgehog (SHH) medulloblastoma (Hovestadt et al., 2014; Kool et al., 2014; Pugh et al., 2012; Robinson et al., 2012), these studies can only be done on advanced tumors and thus they do not illuminate the process of medulloblastoma progression.

Ptch1 heterozygous mice (*Ptch1*$^{+/LacZ}$, designated here as *Ptch1*$^{+/-}$ for simplicity) constitute one of the best-studied models of medulloblastoma (Goodrich et al., 1997). It is currently accepted that medulloblastoma development in *Ptch1*$^{+/-}$ mice is a two-step process in which the *Ptch1*$^{+/-}$ germline mutation leads to preneoplasia formation and the subsequent *Ptch1* loss of heterozygosity (LOH) is sufficient to promote medulloblastoma progression (Ayrault et al., 2009; Pazzaglia et al., 2006). Consistent with this, human genomic studies indicate that medulloblastoma, similar to other pediatric cancers, displays few molecular changes compared to other types of tumors (Pugh et al., 2012). Nevertheless, one study reported that preneoplastic cells with *Ptch1* LOH can differentiate into granule neurons (Kessler et al., 2009), raising the possibility that *Ptch1* LOH is not sufficient to promote medulloblastoma progression and that there may be additional genetic or epigenetic events governing the transition from preneoplasia to medulloblastoma.

Using the *Ptch1* model of medulloblastoma, we discovered that *Ptch1* LOH is a very early event during medulloblastoma development and is associated with high levels of cell senescence in preneoplastic lesions. Additionally, we found that advanced tumors have evaded cell senescence as a result of *p53* mutations or *Cdkn2a* locus inactivation, which occurs via methylation of p16^{Ink4a}/*Cdkn2a* regulatory sequences. Using orthotopic transplantation and genetic experiments, we show that *p53* point mutations prevent cell senescence, accelerate tumor formation, and increase medulloblastoma incidence. Altogether, we propose that medulloblastoma formation requires at least three genetic events, where *p53* or *Cdkn2a* inactivation disables

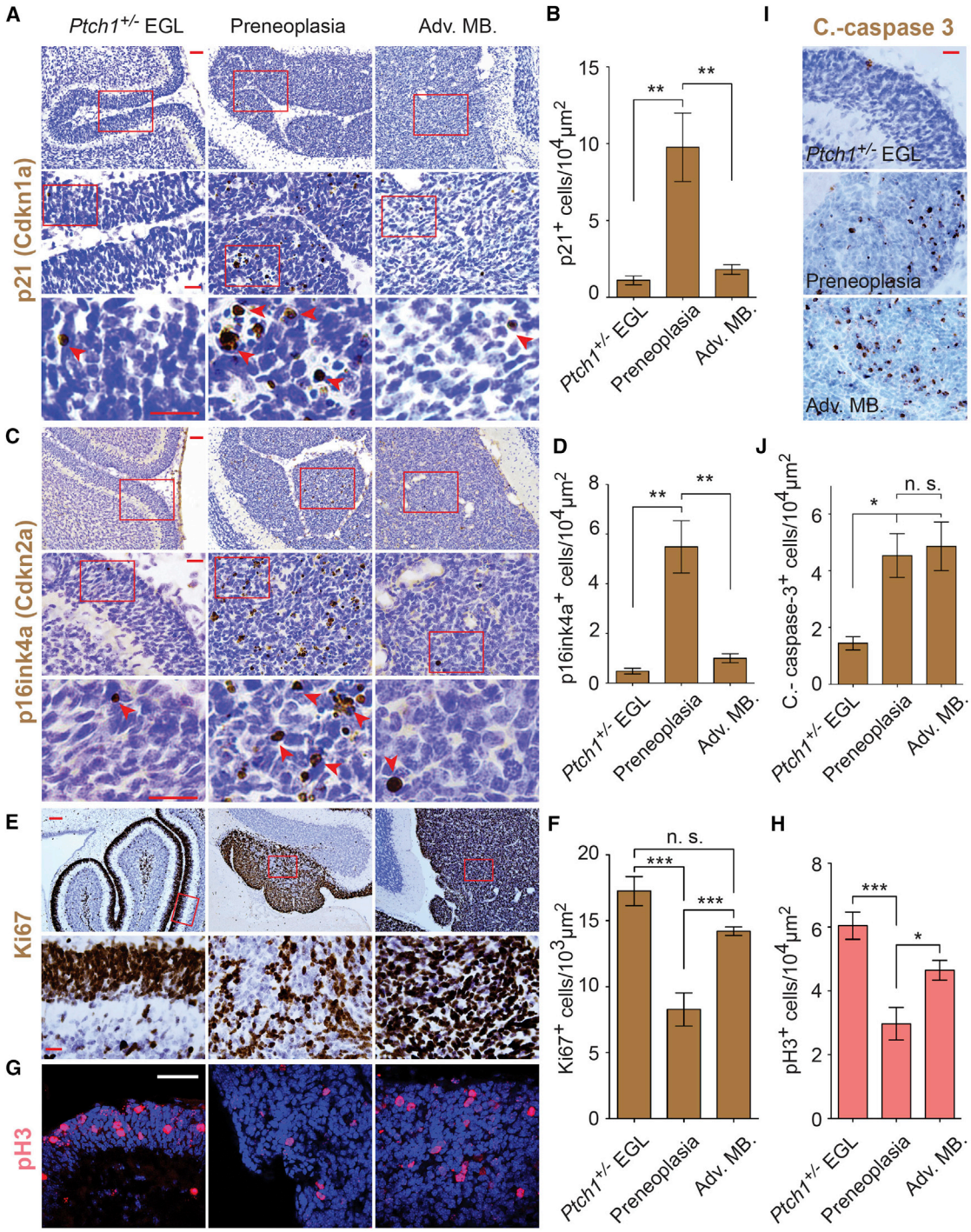

Figure 1. Cell Senescence Is Disabled during Medulloblastoma Progression

(A) p21 (Cdkn1a) immunohistochemistry (IHC) images representative of P7 *Ptch1*$^{+/-}$ EGL, P14 preneoplasia, and advanced medulloblastoma (Adv. MB.).

(B) Number of p21-positive cells per 10,000 μm^2 in *Ptch1*$^{+/-}$ EGL, preneoplasia, and Adv. MB ($n \geq 5$ animals).

(C and D) p16^{Ink4a} IHC staining (C) and (D) number of p16^{Ink4a}-positive cells per 10,000 μm^2 in *Ptch1*$^{+/-}$ EGL, P14 preneoplasia, and Adv. MB (D) ($n \geq 5$ animals). Red arrowheads indicate p21- (A) or p16^{Ink4a}-positive (C) cells.

(E and F) Ki67 IHC staining (E) and number of Ki67^{+} cells in *Ptch1*$^{+/-}$ EGL, P14 preneoplasia, and Adv. MB (F) (n = 6 animals). Red rectangles (A, C, and E) indicate the magnified regions.

(G and H) pH3 immunofluorescence (G) and number of pH3^{+} cells in *Ptch1*$^{+/-}$ EGL, preneoplasia, and Adv. MB (H) (n = 6 animals).

(legend continued on next page)

cell senescence associated with *Ptch1* LOH. Our results also provide a mechanistic explanation for the presence of recurrent inactivation of *TP53* or *CDKN2A* in human SHH medulloblastoma.

RESULTS

Cell Senescence Is Disabled during Medulloblastoma Progression in *Ptch1*$^{+/-}$ Mice

We were puzzled by the fact that while most *Ptch1*$^{+/-}$ mice develop preneoplastic lesions, only a fraction of them acquire advanced medulloblastoma (Mille et al., 2014; Oliver et al., 2005). In some cancers, oncogene activation in precancerous lesions leads to oncogene-induced senescence (OIS), an anticancer mechanism that restrains tumor progression (Braig et al., 2005; Chen et al., 2005; Michaloglou et al., 2005). It is not known whether medulloblastoma precancerous lesions display features of senescence and whether cell senescence plays a tumor-suppressive role during medulloblastoma formation. For example, although *p53* deletion in *Ptch1*$^{+/-}$ mice increases medulloblastoma incidence (Wetmore et al., 2001), the mechanism responsible for this effect was not studied. Similarly, inactivation of important cell-cycle regulators such as p18^{Ink4c} (Uziel et al., 2005) or p27^{Kip1} (Ayrault et al., 2009) increases medulloblastoma incidence in *Ptch1*$^{+/-}$ mice, but the cellular processes responsible for these effects are largely unknown. To test whether cell senescence plays a role during medulloblastoma progression, we assessed the levels of the senescence markers p16^{Ink4a} and p21 at different histopathological stages of medulloblastoma in *Ptch1*$^{+/-}$ mice: postnatal day 7 (P7) external granule-cell layer (EGL), preneoplasia (obtained at P14, the earliest stage preneoplastic lesions can be distinguished), and advanced medulloblastoma (tumors obtained from mice with terminal illness). As expected, the EGL in *Ptch1*$^{+/-}$ cerebella displayed very low levels of p16^{Ink4a} and p21 (Figures 1A–1D and S1C). Interestingly, we found that preneoplastic lesions displayed high numbers of p16^{Ink4a} and p21 positive cells, while advanced medulloblastoma (Adv. MB.) had lost these senescence markers.

We next examined the possible impact of the senescence phenotype on the levels of proliferation at different stages of medulloblastoma. Interestingly, while the EGL and advanced medulloblastoma display a very high proportion of Ki67-positive cells, preneoplastic lesions have more heterogeneous Ki67 staining, with a significantly lower average proliferation (Figures 1E and 1F). We also observed reduced levels of proliferation in preneoplastic lesions using a second proliferation marker, phospho-histone H3 (pH3; Figures 1G and 1H). As expected, cells in preneoplastic lesions that are positive for p16^{Ink4} are negative for proliferation (Figure S1B).

To test whether apoptosis also plays a tumor-suppressive role during medulloblastoma progression, we measured the levels of cleaved-caspase 3 and found that while preneoplastic lesions display higher levels of apoptosis compared to the EGL, advanced medulloblastomas sustain the same levels of apoptosis as preneoplasia, suggesting that apoptosis does not play a major role in limiting the progression from preneoplasia to advanced medulloblastoma (Figures 1I and 1J). Altogether, these results provide evidence that medulloblastoma preneoplastic lesions exhibit a senescent phenotype that negatively impacts their proliferative capacity and may limit their progression to advanced tumors.

p53 Mutations Are Frequent in *Ptch1*$^{+/-}$ Medulloblastoma Displaying *Ptch1* LOH

OIS during cancer development leads to selection pressure for the loss of tumor suppressor genes, such as *TP53*, causing senescence evasion and tumor progression (Narita and Lowe, 2005). Since we observed loss of cell senescence markers at late stages of medulloblastoma, we next looked at the status of *p53* in advanced medulloblastoma tumor samples from *Ptch1*$^{+/-}$ mice. We sequenced the full coding frame of *p53* (exons 2 to 11) and, strikingly, we found *p53* somatic mutations in 36% (7/19) of advanced medulloblastomas (Figures 2A and 2B). Most mutations found were heterozygous missense substitutions located in the p53 DNA binding domain (Figures 2C, 2D, and 2F) that have previously been reported in other cancers and are known to abrogate p53 transcriptional activity and act in a dominant-negative manner (Kato et al., 2003). To determine the status of *Ptch1* in these tumors, we designed a qPCR approach on genomic DNA that detects the wild-type allele of *Ptch1* (Figure 2A). 95% (18/19) of advanced *Ptch1* medulloblastomas display *Ptch1* LOH as a result of a DNA loss (Figure 2A), consistent with previous reports indicating that inactivation of the *Ptch1* wild-type allele is required for medulloblastoma formation (Oliver et al., 2005; Pazzaglia et al., 2006). Importantly, all *p53* mutant tumors also display *Ptch1* LOH (Figure 2A), suggesting that spontaneous *p53* mutations cooperate with *Ptch1* LOH for medulloblastoma development. Overall, the results show that while virtually all advanced *Ptch1* medulloblastomas display *Ptch1* LOH, at least one-third of these tumors also display *p53* inactivation via a mutational mechanism. Therefore, three genetic events are required for medulloblastoma formation in at least one-third of all *Ptch1* medulloblastomas: *Ptch1* heterozygosity, *Ptch1* LOH, and *p53* mutation. These results challenge the idea that *Ptch1* LOH is sufficient for medulloblastoma formation (Pazzaglia et al., 2006).

We next investigated whether other Shh subgroup medulloblastoma mouse models also display spontaneous *p53* mutations. Interestingly, we discovered *p53* mutations in 38% (3/8) of *Olig1-Gnas* murine medulloblastomas (Figure 2E), a mouse model of the Shh subgroup where the Gαs subunit is inactivated in *Olig1*$^{+}$ neuronal progenitors and leads to high levels of

(I and J) Cleaved caspase-3 (C.-caspase 3) IHC staining (I) and number of C.-caspase-3^{+} cells in *Ptch1*$^{+/-}$ EGL, preneoplasia, and Adv. MB (J) (n = 6 animals). 12-μm cryosections were processed for IHC (DAB) and counterstained with cresyl violet (Nissl).

Scale bars in (A)–(C) represent 50 μm (top), 20 μm (middle and bottom); scale bars in (E) represent 200 μm (top) and 20 μm (bottom); scale bars in (G) represent 50 μm; and scale bars in (I) represent 20 μm. Each data point represents the mean number of positive cells/area (per animal) quantified from two or three different randomly selected sections; error bars indicate SEM; one-way ANOVA test with Bonferroni group comparisons was performed (B, D, F, H, and J). >300 cells/section (E and F) and >50 cells/section (A–D) were counted. *, $p \leq 0.05$; **, $p \leq 0.01$; ***, $p \leq 0.001$; n.s., non-significant. See also Figure S1.

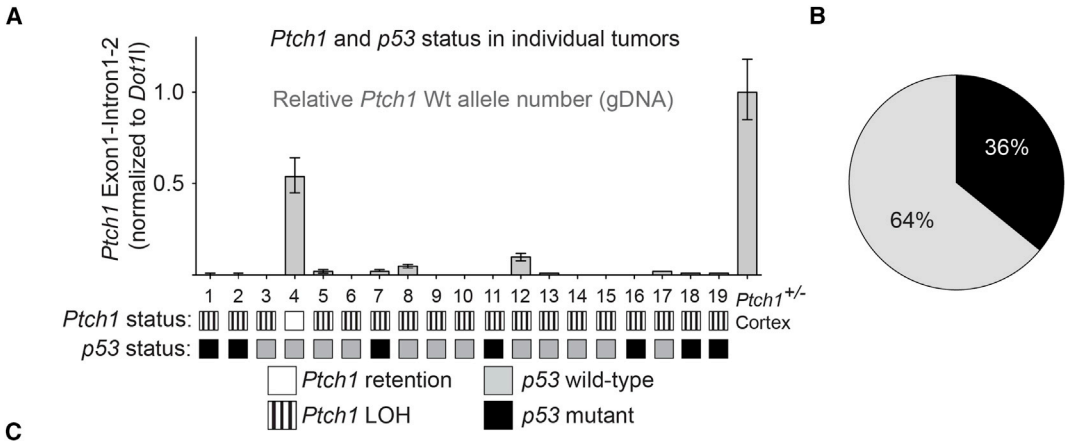

C

Sample	*p53* Mutation		Exon	Type	Somatic counts	Transcriptional activity
	Protein	DNA				
1	p.S238A	c.712T>G	7	missense	12	Non-functional
2	p.R172H	c.515G>A	5	missense	1210	Non-functional
7	p.R245C	c.733C>T	7	missense	1	Not tested
11	p.D278G	c.833A>G	8	missense	17	Non-functional
16	p.R172del;R173S	c.513-515delACG	5	indel	NA	Not tested
18	p.R277K	c.830G>A	8	missense	75	Non-functional
19	p.V213M	c.637G>A	6	missense	80	Non-functional

D

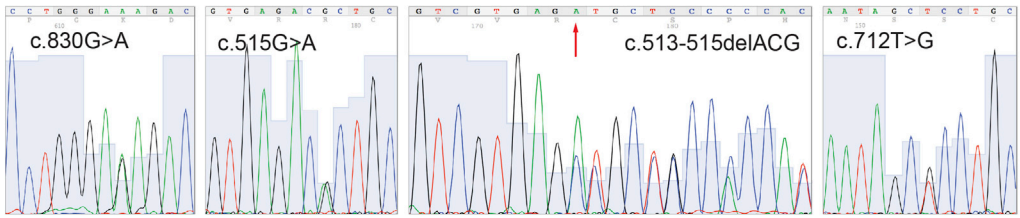

E

Sample (Olig1-Gnas)	*p53* mutation	Exon	Type	Somatic count in human cancer	Transcriptional activity
SRR1550940	p.R172H	5	missense	1210	Non-functional
SRR1550941	p.P275H	8	missense	15	Non-functional
SRR1550944	p.R172H	5	missense	1210	Non-functional

F

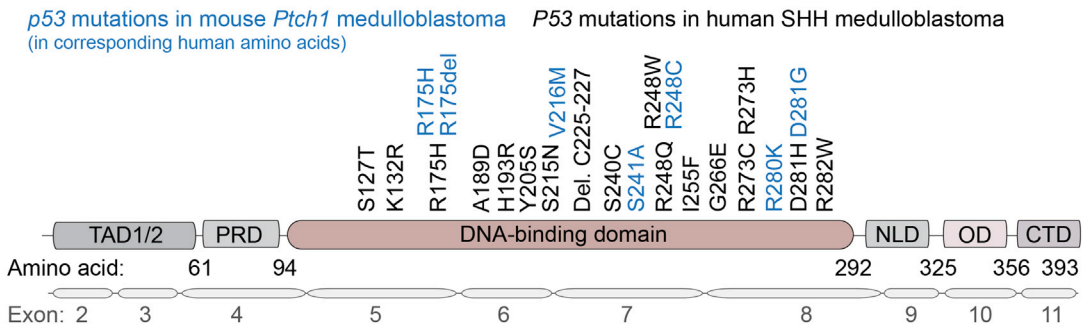

Figure 2. *Ptch1*$^{+/-}$ Medulloblastoma Display *Ptch1* LOH and *p53* Mutations

(A) Histogram showing the status of the *Ptch1* wild-type allele and the *p53* status in Adv. MB. samples. qPCR was performed on gDNA using primers that specifically recognize the *Ptch1* wild-type allele; *Ptch1* wild-type allele number relative to *Dot1l* was normalized to the cortex of *Ptch1*$^{+/-}$ mice (one copy of *Ptch1*). *p53* mutations were identified by Sanger sequencing. Black boxes below each sample indicate *p53* mutations; banded boxes indicate *Ptch1* LOH.

(B) Proportion of medulloblastoma with (black) and without (gray) *p53* mutations.

(C) List of *p53* mutations found in different medulloblastoma samples; columns indicate the protein and DNA description, location of the mutation, type of mutation, number of somatic counts reported in human cancer according to the International Agency for Research on Cancer, and the transcriptional activity of each mutant (Kato et al., 2003).

(D) Examples of chromatograms showing *p53* mutations found in Adv. MB. samples.

(legend continued on next page)

hedgehog signaling (He et al., 2014). Thus, spontaneous *p53* mutations are not only present in the *Ptch1* model but can also be found in other Shh medulloblastoma mouse models.

TP53 mutations have recently been reported in human SHH and WNT primary medulloblastomas (Kool et al., 2014; Zhukova et al., 2013). Interestingly, the frequency of *p53* mutations in the *Ptch1* and *Olig1-Gnas* mouse models and in human SHH medulloblastomas is comparable (36%–38% in mice versus 13%–21% in humans); moreover, the nature of the *P53* mutations and their location in the *TP53* gene are remarkably similar (Figure 2F).

p53 Pathway Dysfunction in a Large Proportion of Advanced Medulloblastoma

Since mutations that compromise the P53 pathway are frequent in human medulloblastoma (Kool et al., 2014), we investigated whether some *Ptch1* medulloblastomas that do not bear *p53* mutations also exhibit deregulation of the p53 pathway. *p53* mutations alter p53 transcriptional activity and lead to p53 protein accumulation because *p53* mutants can no longer induce the expression of its negative regulator *Mdm2*. As expected, when we assessed p53 levels in $Ptch1^{+/-}$ medulloblastomas, we found nuclear accumulation of p53 in all advanced tumors bearing missense *p53* mutations (Figure S2A). Remarkably, we also found p53 nuclear accumulation in 50% (3/6) of *p53* wild-type medulloblastomas, indicating that the p53 pathway is also altered in tumors without *p53* mutations.

To further test whether p53 signaling is dysfunctional in advanced medulloblastomas, we evaluated the integrity of p53 transcriptional activity in response to UV radiation in tumor cells freshly isolated from primary $Ptch1^{+/-}$ medulloblastomas with and without *p53* somatic mutations. We assessed p53 activity by measuring the mRNA levels of the p53 targets *Pai-1*, *p21*, and *Noxa*. As expected, *p53* mutant medulloblastoma cells were deficient in upregulating *Pai-1*, *p21*, and *Noxa* in response to UV (Figure S2B). Interestingly, while many *p53* wild-type tumors were capable of strongly activating these p53 target genes, 50% (7/14) of *p53* wild-type tumors were deficient in transactivating these key p53 target genes in response to UV (tumors below the median dashed line in Figure S2C and encircled in Figure S2B). Furthermore, when plotted to simultaneously compare the expression of these three p53 targets, many *p53* wild-type tumors behave similarly to *p53* mutant tumors (Figure S2D). Therefore, one-half of *p53* wild-type medulloblastomas display p53 signaling defects.

Ptch1 LOH Precedes *p53* Mutations during Medulloblastoma Formation

If, as our data suggest, *p53* mutations occur to evade cell senescence in preneoplastic cells, *p53* mutations should occur after *Ptch1* LOH. To test this hypothesis, we determined the temporal order in which *Ptch1* LOH and *p53* mutations occur during medulloblastoma formation in $Ptch1^{+/-}$ mice. Using laser-capture microdissection (LCM), we isolated genomic DNA from preneoplastic lesions to sequence *p53* and assess the status of *Ptch1* (Figures 3A and 3B). While the internal granule-cell layer (IGL) of the cerebellum retained one allele of *Ptch1*, preneoplastic lesions had a clear absence of the *Ptch1* wild-type allele (Figure 3B). To assess whether we could reliably determine the presence of *p53* mutations from microdissected tissue, we laser-captured tissue from advanced medulloblastoma samples in which we previously found *p53* mutations; when we sequenced *p53* from these samples, we obtained sequences where the p53 mutations were readily identifiable (Figure 3C). When we microdissected a cohort of P14 preneoplastic lesions, we found that 10 out of 14 (71%) preneoplastic lesions displayed *Ptch1* LOH. Interestingly, none of the preneoplastic lesions at P14 had *p53* mutations (Figure 3D), indicating that *Ptch1* LOH precedes *p53* mutations. Consistent with this, when we immunostained preneoplastic lesions for p53, we did not find nuclear accumulation of p53 (Figure 3E), supporting the idea that the p53 pathway is not deregulated at this stage of medulloblastoma.

p53 Mutations Prevent *Ptch1* LOH-Dependent Senescence and Accelerate Medulloblastoma Formation

In our analysis of medulloblastoma progression, high levels of senescence correlate with *Ptch1* LOH, while *p53* mutations correlate with the loss of the senescence phenotype. To mechanistically assess whether *p53* mutations can bypass cell senescence during medulloblastoma progression, we used an orthotopic transplantation approach where $Ptch1^{+/-}$ granule cell precursors (GCPs) isolated at P7 were transduced with a lentivirus encoding $p53^{R270C}$ (or *GFP*, as a control) and then rapidly implanted into the cerebella of C57Bl6 mice at P7 to mimic their normal cerebellar microenvironment (Figure 4A). Transplanted $Ptch1^{+/-}$ GCPs can be detected by their expression of β-galactosidase, due to the insertion of the *lacZ* gene into the *Ptch1* locus. When we dissected the cerebella 6 weeks after injection, we observed that $p53^{R270C}$ lesions were significantly bigger compared to their *GFP* controls (Figures 4B and 4C). We confirmed that $p53^{R270C}$ lesions still expressed the *p53* mutation even after 6 weeks (Figure 4D). Both *GFP* and $p53^{R270C}$ tumors displayed *Ptch1* LOH, indicating that *p53* mutations are not responsible for *Ptch1* LOH (Figure 4E). Importantly, the levels of cell senescence as assessed by the number of $p16^{Ink4a}$-positive cells were lower in the presence of the *p53* mutation (Figure 4F). Strikingly, introduction of the $p53^{R270C}$ mutation dramatically accelerated medulloblastoma formation and increased tumor incidence (Figure 4G). Together, these results indicate that *p53* mutations during medulloblastoma formation bypass the cell senescence associated with *Ptch1* LOH

(E) List of *p53* mutations discovered in *Olig1-Gnas* medulloblastoma.
(F) Schematic structure of the P53 protein displaying the location of the *p53* mutations found in *Ptch1* mouse medulloblastoma (blue) as well as the *TP53* mutations reported in human SHH medulloblastoma (black) by Zhukova et al. (2013). TAD1/2, transactivation domain; PRD, proline-rich domain; NLD, nuclear localization domain; OD, oligomerization domain; CTD, C-terminal domain.
See also Table S1 and Figure S2.

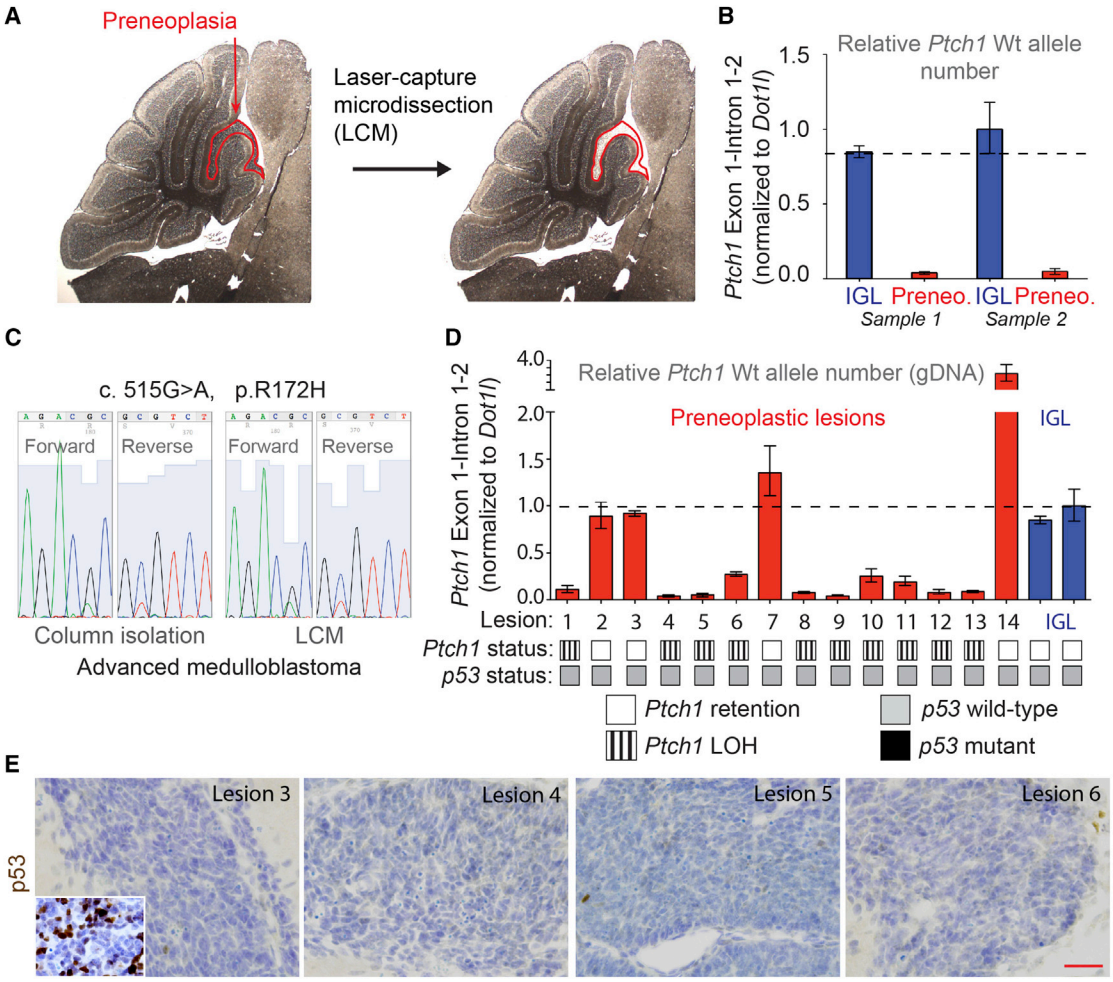

Figure 3. *Ptch1* LOH Precedes *p53* Mutations during MB Formation

(A) Laser-capture microdissection (LCM) of medulloblastoma preneoplastic lesions. A P14 cerebellum section where a preneoplastic lesion (red) is indicated (left). After microdissection, the region is captured (right).

(B) The IGL from P14 $Ptch1^{+/-}$ cerebella shows retention of the *Ptch1* wild-type allele (one copy), while preneoplastic lesions have lost the *Ptch1* wild-type allele.

(C) Sanger sequences of DNA from an advanced medulloblastoma isolated using a standard DNA isolation column from a piece of tumor (left) or from a tissue section of the same tumor using LCM (right); in both cases, the mutation can be readily identified.

(D) Histogram showing the absence or presence of the *Ptch1* wild-type allele in P14 preneoplastic lesions. qPCR was performed on genomic DNA isolated from each microdissected lesion. *Ptch1* wild-type allele number relative to *Dot1l* was normalized to the IGL of $Ptch1^{+/-}$ mice (one copy of *Ptch1*). The *Ptch1* status and *p53* status is indicated below the graph; white squares indicate *Ptch1* retention while striped squares indicate *Ptch1* LOH; gray squares indicate *p53* wild-type sequences.

(E) p53 IHC on preneoplastic lesions shows absence of nuclear accumulation of p53 protein. Inset shows an Adv. MB. sample as positive control. Numbers indicate the corresponding lesions from Figure 3D. Scale bar, 40 μm.

in preneoplastic lesions, thus accelerating medulloblastoma progression.

To extend our orthotopic transplantation findings with an entirely genetic model, we also generated $Ptch1^{+/-}$ mice carrying the conditional $p53^{R172H}$ mutant allele (Olive et al., 2004). This allele corresponds to one of the sporadic *p53* mutations found in our medulloblastoma cohort (Figure 2C). Since the conversion of the conditional *p53* locus to the $p53^{R172H}$ allele is Cre dependent, we used the *Math1-Cre* transgene to induce recombination (referred to as $Ptch1^{+/-}$;$p53^{+/R172H}$). We found that expression of the $p53^{R172H}$ mutation in the cerebellum accelerates medulloblastoma formation and increases medulloblastoma incidence in $Ptch1^{+/-}$ mice (Figure 4H). Advantageously, as the $p53^{R172H}$ mutation is a knockin, expression of $p53^{R172H}$ in these experiments is controlled by its endogenous promoter. Furthermore, as previous medulloblastoma p53 studies have always used a null *p53* allele, this is the first time that a *p53* point mutation is shown to collaborate with $Ptch1^{+/-}$ in medulloblastoma. Importantly, the fact that $Ptch1^{+/-}$;$p53^{+/R172H}$ has a stronger effect than $Ptch1^{+/-}$;$p53^{+/-}$ demonstrates that this mutation is not a simple null mutation but rather acts as a dominant-negative and/or gain-of-function

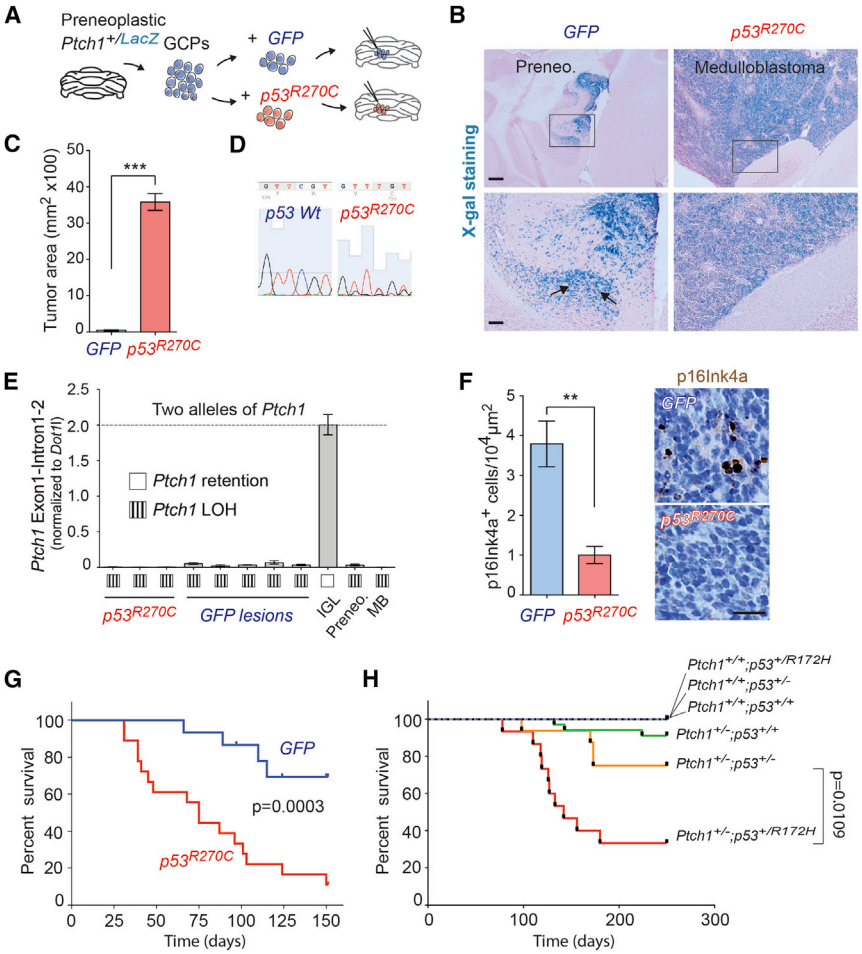

Figure 4. *p53* Mutations Prevent *Ptch1* LOH-Dependent Cell Senescence and Accelerate Tumor Progression

(A) Diagram depicting the orthotopic transplantation approach where preneoplastic *Ptch1*$^{+/lacZ}$ GCPs were transduced by spin-inoculation with either a *GFP* or a *p53*^{R70C} lentivirus before transplantation.

(B) X-gal stainings to detect lesions 6 weeks after transplantation. *GFP*$^{+}$ lesions were smaller and frequently display regions of differentiated granule neurons populating the IGL (arrows), while *p53*^{R70C} lesions correspond to Adv. MBs that do not display features of differentiation. Scale bars represent 200 μm (top) and 50 μm (bottom). Bottom pictures are magnified regions indicated by the black boxes.

(C) Tumor area of *GFP* and *p53*^{R70C} lesions (n ≥ 4).

(D) Chromatograms of wild-type *p53* or the *p53*^{R70C} mutation isolated from advanced *p53*^{R70C} tumors.

(E) Histogram showing the status of the *Ptch1* wild-type allele in *GFP* and *p53*^{R70C} lesions. *Ptch1* wild-type allele number relative to *Dot1l* was normalized to the IGL of the *Ptch1*$^{+/+}$ recipient mice (two copies of *Ptch1*).

(F) Number of p16^{Ink4a}-positive cells in *GFP* lesions compared to *p53*^{R70C} tumors (n ≥ 4) and examples of p16^{ink4a} IHC pictures; scale bar, 20 μm.

(G) Kaplan-Meier survival analysis of C56BL6 mice that received cerebellar transplants of preneoplastic GCPs infected with *p53*^{R70C} (red) or *GFP* (blue).

(H) Survival analysis of *Ptch1*$^{+/-}$;*p53*$^{+/R172H}$, *Ptch1*$^{+/-}$;*p53*$^{+/-}$, *Ptch1*$^{+/-}$;*p53*$^{+/+}$, and *Ptch1*$^{+/+}$ control mice showing that the *p53*^{R172H} mutant allele accelerates medulloblastoma formation and increases medulloblastoma incidence in *Ptch1*$^{+/-}$ mice.

U test performed in (C) and Student's t test in (F). Error bars indicate SEM. Log-rank test was performed in (G) and (H).

mutant. Thus, this new mechanistic result supports and further extends the conclusions of our orthotopic transplantation experiments.

p16^{ink4a} Inactivation Is an Alternative Mechanism for Cell Senescence Evasion during Medulloblastoma Progression

After finding that spontaneous *p53* mutations explain senescence evasion in one-third of medulloblastoma, we next assessed possible alternative mechanisms to p53 inactivation that could also lead to senescence evasion. The *Cdkn2a* locus is comprised of two transcripts: *p16*^{ink4a} and *Arf*. The loss of either of these transcripts, similarly to mutations in *p53*, can lead to senescence evasion in other cancers (Carnero et al., 2000; Michaloglou et al., 2005). However, since the *Arf* knockout neither accelerates *Ptch1*$^{+/-}$ medulloblastoma formation nor increases its incidence (Wetmore et al., 2001), we focused on *p16*^{ink4a} as a possible alternative mechanism to p53 inactivation resulting in senescence evasion.

We first quantified the mRNA expression of *p16*^{ink4a} and found that 60% (6/10) of the advanced medulloblastomas without *p53* mutations have low expression of *p16*^{ink4a} mRNA (Figure 5A; samples with *p16*^{ink4a} expression lower than 50% of the mean [dotted line] are defined as *p16*^{ink4a} low). We next investigated the mechanism leading to this low expression of *p16*^{ink4a}. We did not detect gene copy-number changes in *p16*^{ink4a} (exon 1α of *Cdkn2a*) (Figure 5B); in addition, we did not find *p16*^{ink4a} mutations. Interestingly, using bisulfite sequencing, we found *p16*^{ink4a} promoter/regulatory sequence methylation (Figure 5C) in most advanced medulloblastoma samples with low *p16*^{ink4a} expression (5/6; Figure 5D). Conversely, in the majority of medulloblastoma presenting unmethylated *p16*^{ink4a} promoter (3/4), *p16*^{ink4a} expression was high (Figure 5D). Consistently, advanced medulloblastomas with *p16*^{ink4a} promoter methylation display lower *p16*^{ink4a} mRNA expression compared with samples without promoter methylation (Figure 5E), and the levels of *p16*^{ink4a} promoter methylation are negatively correlated with *p16*^{ink4a} expression (Figure 5F). As downregulation of *p16*^{ink4a}/*Cdkn2a* causes senescence evasion in many cancers (Michaloglou et al., 2005), methylation of the *p16*^{ink4a} promoter, leading to its low expression in many advanced medulloblastomas, is likely to be a major determinant of their ability to have evaded senescence.

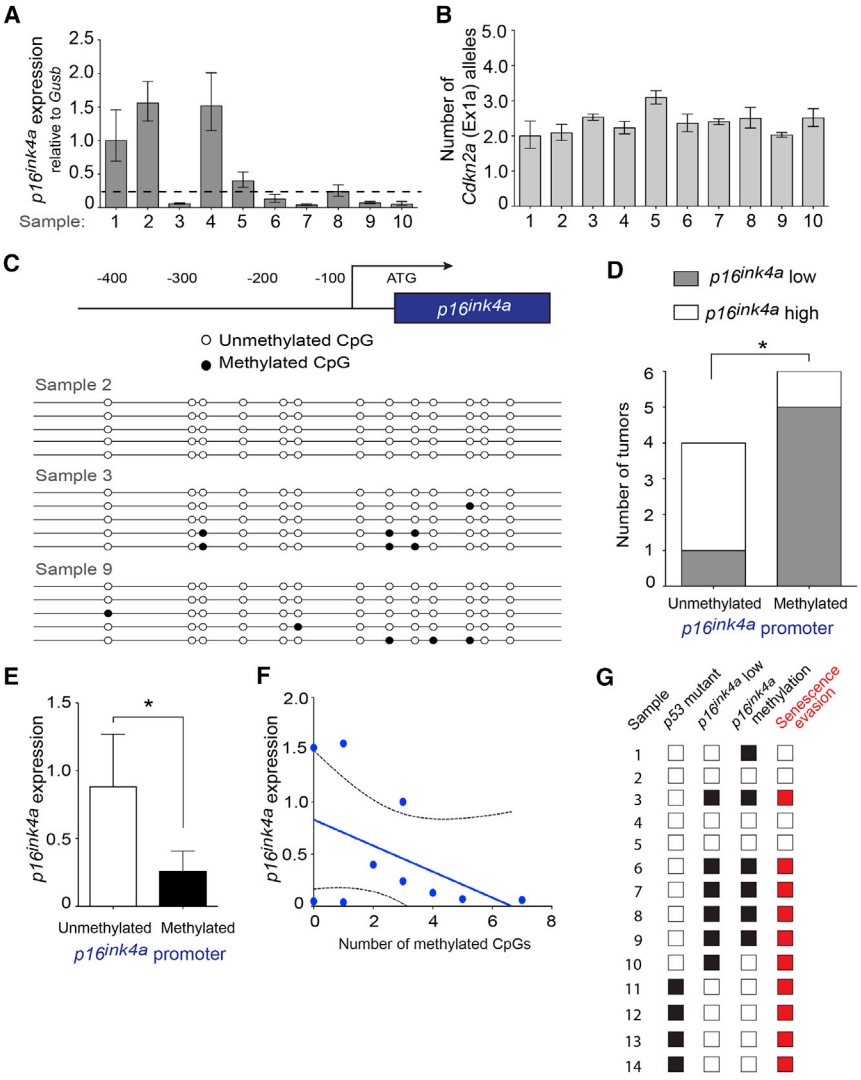

Figure 5. *p16*^{ink4a} Promoter Methylation Leads to *p16*^{ink4a} Loss of Expression in Advanced Medulloblastoma

(A) *p16*^{ink4a} mRNA expression levels relative to *Gusb* in 10 advanced medulloblastomas without *p53* mutations. 60% of *p53* wild-type medulloblastomas display loss of *p16*^{ink4a} expression.

(B) Copy-number analysis of the *Cdkn2a* exon 1α. qPCR was performed using gDNA as template; *Cdkn2a* exon 1α levels relative to *Dot1l* are shown.

(C) Schematics of the *p16*^{ink4a} promoter region and lollipop representation of *p16*^{ink4a} promoter/regulatory sequence methylation in three representative tumor samples from (A); methylated and unmethylated CpGs are represented as black circles or empty circles, respectively.

(D) Correlation between *p16*^{ink4a} promoter methylation and *p16*^{ink4a} mRNA expression; chi-square test was performed.

(E) *p16*^{ink4a} mRNA expression levels relative to *Gusb* in medulloblastomas according the methylation status of their *p16*^{ink4a} promoter. Medulloblastomas with *p16*^{ink4a} promoter methylation display low *p16*^{ink4a} mRNA expression compared to unmethylated samples (one-tailed t test).

(F) Correlation between methylation levels (number of methylated CpGs) and *p16*^{ink4a} expression.

(G) *p53* status, *p16*^{ink4a} expression and *p16*^{ink4a} promoter methylation status in 14 advanced medulloblastomas. Black boxes indicate *p53* mutations, low *p16*^{ink4a} expression and *p16*^{ink4a} promoter methylation. Senescence evasion (red boxes) was determined when a tumor had either a *p53* mutation or *p16*^{ink4a} inactivation.

*, $p \leq 0.05$; **, $p \leq 0.01$; ***, $p \leq 0.001$; n.s., non-significant.

We also investigated the relevance of these findings to human medulloblastoma. We found that a subset (22%) of human SHH medulloblastoma has higher *p16*^{INK4A} regulatory sequence methylation than the bulk of SHH medulloblastoma and normal cerebellum (Figure 6A). Similar to our mouse data, methylation of human *p16*^{INK4A} correlates with its low expression in medulloblastoma ($p = 0.0398$), suggesting that the mechanism of *p16*^{ink4a} regulation that we describe here for mice might also apply to human medulloblastoma.

Interestingly, we also found that ~4% of human SHH medulloblastomas have a loss of the *CDKN2A* gene (Figure 6B; see tumors below the red line). This loss is subgroup specific, indicating that there is selection for the inactivation of *CDKN2A* in SHH medulloblastoma. A closer inspection of the deleted regions identified that some medulloblastomas harbor focal loss of *CDKN2A* (Figure 6C). In addition to *CDKN2A* gene loss, a deleterious point mutation has also been reported in *CDKN2A* in SHH medulloblastoma (Kool et al., 2014). This mutation (R80X) is predicted to affect the function of p16INK4A, but not ARF (Quelle et al., 1997), further supporting a role for p16INK4A, but not ARF, in SHH medulloblastoma. Importantly, these results in human tumors further support the functional relevance of our finding that *p16*^{ink4a}/*Cdkn2a* downregulation plays a role in medulloblastoma progression.

DISCUSSION

Senescence Evasion Is a Hallmark of Medulloblastoma

It was previously demonstrated that *Ptch1* heterozygosity leads to GCP overproliferation and the formation of a hyperplastic EGL, the first detectable histopathological stage of medulloblastoma (Thomas et al., 2009). Using *Ptch1*$^{+/-}$ mice we found that *Ptch1* LOH is a very early event during medulloblastoma formation, associated with high levels of cell senescence in preneoplastic lesions (Figure 7). We propose that hyper-activation of hedgehog signaling due to *Ptch1* LOH creates high levels of oncogenic stress in preneoplasia, leading to OIS, an anticancer mechanism that restrains the progression from preneoplasia to advanced medulloblastoma (Figure 7). We found that *p53* mutations or p53 pathway deregulation are frequent in advanced tumors, and we discovered that *p53* mutations appear after

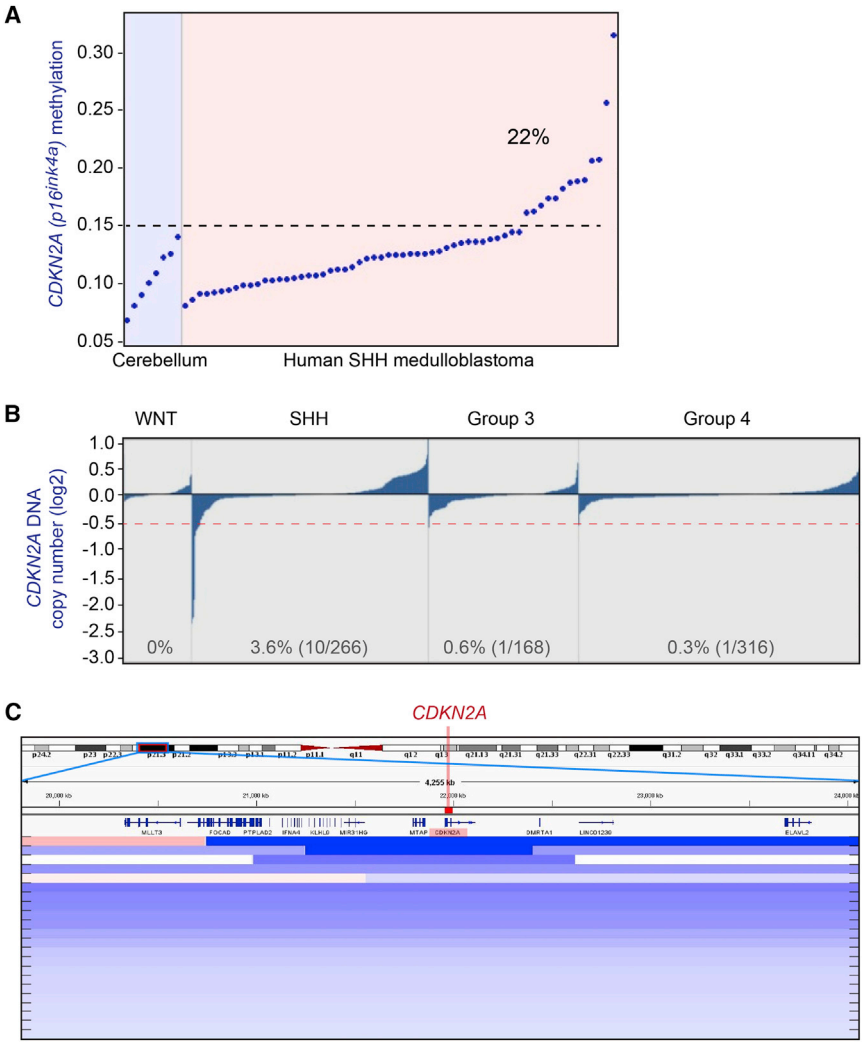

Figure 6. *CDKN2A* Locus Alterations in Human SHH Medulloblastoma

(A) *CDKN2A* methylation at a $p16^{ink4a}$ regulatory region in SHH human medulloblastoma samples.

(B) Gene copy-number changes in the human *CDKN2A* locus in medulloblastoma, according to the molecular subtype. Percentage of tumors with *CDKN2A* loss is indicated.

(C) Focal genomic losses encompassing the *CDKN2A* locus. The location of *CDKN2A* is indicated on human chromosome 9 (top); this magnified region (bottom) comprises 4.3 Mb. The *CDKN2A* gene is indicated with a red line in the middle of the magnified region. Blue horizontal lines indicate genomic losses, with darker blue intensity reflecting higher copy-number loss.

Ptch1 LOH, supporting the idea that cell senescence during preneoplastic stages creates a selection pressure for the loss of p53 function. Accordingly, we demonstrate that introducing a *p53* mutation bypasses cell senescence and accelerates medulloblastoma formation. Additionally, many medulloblastomas without *p53* mutations display $p16^{ink4a}$ promoter methylation and low $p16^{ink4a}$ expression (Figure 5G), an alternative mechanism known to lead to senescence evasion. Therefore, we propose that *p53* mutations or *Cdkn2a* inactivation constitute a third hit to evade cell senescence subsequent to *Ptch1* LOH. Together, *p53* mutations (found in 36% of tumors) and *Cdkn2a* inactivation (60% of the non-*p53* mutated [100% − 36% = 64%] are *Cdkn2a* low [38%]) explain senescence evasion in 74% of advanced medulloblastoma. Interestingly, we found that 64% of human SHH medulloblastomas display mutations that compromise the integrity of the P53 or CDKN2A pathway (Table S1). Importantly, a genome-wide functional screen for genes that collaborate with $Ptch1^{+/-}$ in mouse medulloblastoma formation identified seven insertion mutations in the *Cdkn2a* locus in 85 tumors ($p = 0.0067$), indicating that *Cdkn2a* mutations collaborate with $Ptch1^{+/-}$ and supporting a functional role for the inactivation of *CDKN2A* in SHH medulloblastoma (Genovesi et al., 2013). Overall, these data suggest that P53 or CDKN2A pathway inactivation plays an essential role in the development of murine and human SHH medulloblastoma.

Importantly, while it has been previously shown that targeted inactivation of *p53* can accelerate medulloblastoma formation in $Ptch1^{+/-}$ mice and increase its incidence (Wetmore et al., 2001), it remained unknown whether *p53* mutations were involved in the natural history of medulloblastoma. Thus, our study uncovers a new mechanism about the genomic progression of medulloblastoma.

Notably, our results also indicate that *Ptch1* LOH is not the genetic event that governs the transition from preneoplasia to neoplasia and that *Ptch1* LOH is not sufficient for medulloblastoma formation, as was previously thought (Pazzaglia et al., 2006). This finding is consistent with what has been suggested by others (Kessler et al., 2009; Oliver et al., 2005), although additional events have never been demonstrated. Therefore, medulloblastoma progression may not be as simple as other two-hit cancer models such as retinoblastoma and displays similarities to epithelial cancers, where multiple genetic events are required for tumor formation and *p53* mutations tend to be a late event (Fearon and Vogelstein, 1990).

Hedgehog and p53 Signaling in Medulloblastoma

Shh signaling downregulates p53 activity (Stecca and Ruiz i Altaba, 2009), possibly by Gli1 activation of Mdm2 (Abe et al., 2008). Consistent with this, reducing levels of Mdm2 increase p53 levels and lead to cerebellar hypoplasia and reduced medulloblastoma development in $Ptch1^{+/-}$ mice (Malek et al., 2011), implying that p53 signaling is essential for medulloblastoma tumor suppression. Similarly, the proto-oncogene PPM1D, a negative regulator of P53, is overexpressed in medulloblastomas

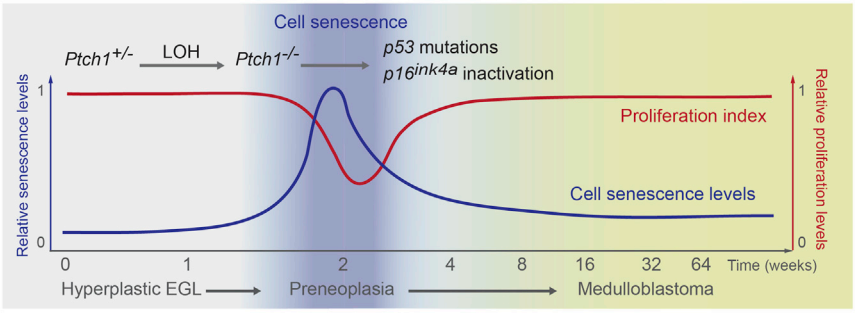

Figure 7. Senescence Is a Barrier for Medulloblastoma Progression

There are three histopathological stages of medulloblastoma in *Ptch1*$^{+/-}$ mice: hyperplastic EGL, preneoplasia, and advanced medulloblastoma. Preneoplastic lesions display high levels of cell senescence and low levels of proliferation, changes associated with *Ptch1* LOH. Advanced medulloblastomas display *p53* mutations, deregulated p53 signaling, or *p16*^{ink4a} promoter methylation, events that allow escape from cell senescence and lead to progression from preneoplasia to medulloblastoma. The x axis indicates time, and the y axis indicates the relative levels of cell senescence (left axis) and proliferation (right axis) according to the experimental data from Figure 1.

(Castellino et al., 2008) and increases medulloblastoma formation in mice when overexpressed together with Shh (Doucette et al., 2012). Together, these findings provide strong evidence that hedgehog signaling leads to a functional inactivation of p53 signaling to permit GCP proliferation and, in some instances, medulloblastoma formation. However, the presence of somatic *p53* mutations in *Ptch1*$^{+/-}$ medulloblastoma (this study) demonstrates that the ability of Shh signaling to functionally suppress p53 signaling is not always sufficient to inactivate p53 activity in a tumorigenic context.

TP53 Mutations in Human SHH Medulloblastoma

Recently, it has been reported that the frequency of *TP53* mutations in the WNT and SHH medulloblastoma subgroups is 16% and 21%, respectively, but they are absent from group 3 and 4 medulloblastoma (Zhukova et al., 2013). Since most cases of human SHH medulloblastoma with *TP53* mutations also display mutations affecting hedgehog signaling (Kool et al., 2014), these studies indicate that specific molecular mechanisms occurring in SHH medulloblastoma lead to selection pressure for the inactivation of the P53 pathway. Based on our results, we propose that cell senescence resulting from overactive hedgehog signaling constitutes a tumor-suppressive mechanism in medulloblastoma that leads to *TP53* mutations during medulloblastoma progression. Because it is virtually impossible to analyze preneoplastic stages in human, and because the molecular analysis of advanced tumors does not allow the establishment of the temporal sequence in which mutations arise during tumor formation, our study indicates that in medulloblastoma cases with somatic *TP53* mutations, these somatic *TP53* mutation events likely occur at late stages of medulloblastoma formation.

In addition to the somatic mutations, close to 50% of *TP53* mutations in SHH medulloblastoma are germline mutations (Kool et al., 2014; Zhukova et al., 2013); patients with Li-Fraumeni syndrome develop exclusively SHH medulloblastomas as a result of chromothriptic events that lead to mutations in hedgehog signaling components (Rausch et al., 2012). This demonstrates that in Li-Fraumeni syndrome, mutations in hedgehog signaling genes can occur after *TP53* mutations and lead to SHH medulloblastoma formation. Although *p53* knockout mice or mouse models of Li-Fraumeni syndrome seldom develop medulloblastoma (Olive et al., 2004), the combined inactivation of *p53* and DNA repair factors lead to medulloblastomas of the Shh subgroup that harbor chromosomal deletions encompassing the *Ptch1* locus (Frappart et al., 2009). Therefore, evidence from both mouse and human studies supports two different molecular mechanisms of medulloblastoma formation where p53 mutations can occur before or after mutations in hedgehog signaling components. When happening first, mutations in hedgehog signaling components lead to cell senescence and are followed by *p53* inactivation (Figure 7); in contrast, *TP53* germline mutations cause chromosomal instability and lead to mutations in hedgehog signaling genes.

Apoptosis and Medulloblastoma Tumor Suppression

It has been recently reported that mis-expression of N-Myc in neuronal progenitors (referred to as the GTML tumor model) leads to the formation of medulloblastomas that harbor somatic *p53* mutations (Hill et al., 2015), indicating that *p53* mutations collaborate with N-Myc overexpression for medulloblastoma formation. GTML tumors have a signature of group 3 medulloblastoma and represent a model for medulloblastoma relapse cases with combined *c-MYC* or *N-MYC* and *TP53* mutations (Hill et al., 2015). Interestingly, overexpression of c-Myc in GCPs (Kawauchi et al., 2012) or in CD133^{+} neural stem cells (Pei et al., 2012) gives origin to aggressive group 3 medulloblastoma only in combination with *p53* inactivation, while c-Myc overexpression alone only leads to the formation of hyperplasia, which likely regress as a result of p53-dependent apoptosis (Pei et al., 2012). Therefore, the available evidence suggests that P53 pathway inactivation might also be required for group 3 medulloblastoma development and that p53-dependent apoptosis may be one of the tumor-suppressive mechanisms in this medulloblastoma subgroup. Importantly, the molecular mechanisms leading to the acquisition of somatic *p53* mutations in tumors overexpressing N-Myc have not been explored (Hill et al., 2015).

In models of Shh medulloblastoma, there is little evidence that apoptosis is a strong tumor-suppressive mechanism. *Ptch1* has been suggested to act as a proapoptotic dependence receptor in the developing spinal cord that leads to caspase-9 activation in absence of the ligand Shh (Mille et al., 2009). According to this, the absence of *Ptch1* in preneoplasia should lead to reduced levels of apoptosis compared to the EGL; however, we observed higher levels of apoptosis in preneoplasia compared to the EGL (Figures 1I and 1J). While the reason for this is not clear, it could

be due to tissue-specific differences between spinal cord and cerebellum.

The fact that we did not observe changes in apoptosis levels as preneoplastic lesions progress from preneoplasia to advanced medulloblastoma (Figures 1I and 1J) supports the notion that apoptosis is not an essential tumor-suppressive barrier to Shh medulloblastoma progression. Consistent with this, human SHH medulloblastomas display a paucity of mutations involved in apoptosis (Kool et al., 2014). Therefore, cell senescence appears to be a more important tumor-suppressive mechanism than apoptosis for Shh medulloblastoma, while the converse might be true for group 3 medulloblastoma. Consistent with this, *p53* mutations are known to have context-specific effects. For example, it has been shown that in tumors such as lymphomas *p53* mutations abrogate apoptosis but not cell senescence, while in sarcomas *p53* mutations abrogate cell senescence but not apoptosis (Ventura et al., 2007). The fact that p53 dysfunction does not reduce apoptosis in Shh medulloblastoma suggests that p53 preferentially regulates cell senescence over apoptosis in these tumors.

Cell Senescence Is a Tumor-Suppressive Mechanism for Medulloblastoma

Here, we provide evidence that medulloblastoma preneoplastic lesions display a senescent phenotype that limits their proliferative capacity and their progression to advanced tumors. Although we describe this senescence response as a form of OIS, cell senescence in medulloblastoma preneoplasia likely results from the oncogenic stress subsequent to the loss of *Ptch1*, a tumor suppressor gene; analogously, loss of PTEN, another tumor suppressor, has been shown to induce senescence in prostate cancer (Chen et al., 2005). Loss of *Ptch1* leads to hyperactivation of hedgehog signaling, which can lead to high levels of N-Myc and CyclinD1, two candidates that can mediate *Ptch1* LOH-dependent oncogenic stress and senescence. Because Ptch1 has also been shown to interact with and to sequester CyclinB1 at the cell membrane (Barnes et al., 2001), the increased nuclear availability of CyclinB1 after *Ptch1* LOH may also lead to oncogenic stress.

Basal cell carcinoma (BCC), a skin tumor caused by deregulation of hedgehog signaling, is characterized by mutations in *PTCH1* (Gailani et al., 1996). Similar to medulloblastoma, *PTCH1* LOH is required for BCC formation (Gailani et al., 1996). Importantly, *TP53* mutations occur in BCCs together with *PTCH1* mutations (Zhang et al., 2001) even in the presence of *PTCH1* LOH. This indicates that p53 pathway inactivation also cooperates with hedgehog signaling deregulation during BCC formation. However, whether *TP53* mutations precede or follow *PTCH1* LOH in BCC remains unknown (Ling et al., 2001). In view of our data, we speculate that at least in some cases, BCC preneoplastic lesions may experience cell senescence, leading to P53 inactivation.

In conclusion, our data suggest that cell senescence in medulloblastoma preneoplastic lesions creates selection pressure for p53 and p16ink4a inactivation. We propose that human SHH medulloblastomas as well as BCCs with *PTCH1* mutations may experience similar molecular changes that also lead to *TP53* mutations and senescence evasion. In addition to *TP53* and *CDKN2A*, mutations in other genes important for cell senescence such as *P63* and *ATM* have also been reported in SHH medulloblastoma (Kool et al., 2014), further supporting the idea that cell senescence constitutes a tumorigenesis barrier during medulloblastoma precancerous stages.

EXPERIMENTAL PROCEDURES

Additional experimental procedures for qRT-PCR, bioinformatic analyses, virus preparation, orthotopic transplantation, and bisulfite sequencing can be found in Supplemental Experimental Procedures.

Mouse Lines

All animal work was performed according to the Canadian Council on Animal Care guidelines. $Ptch1^{+/lacZ}$ (referred to as $Ptch1^{+/-}$) mice (Goodrich et al., 1997) were backcrossed with C57BL/6 mice (Harlan). $p53^{R172H}$ mutant mice ($p53^{LSL\text{-}R172H}$) were described previously (Olive et al., 2004).

Immunohistochemistry

12-μm cryosections were processed for immunohistochemistry or immunofluorescence as described previously (Izzi et al., 2011; Mille et al., 2014). Antibodies and dilutions are described in Supplemental Experimental Procedures.

p53 sequencing

To screen for *p53* mutations, we isolated genomic DNA from advanced medulloblastomas and sequenced the full coding frame of the *p53* gene. Each sequence was inspected to find mutations. Indels were detected using CodonCode Aligner. See Supplemental Experimental Procedures for primer sequences.

Laser Capture Microdissection

Preneoplastic lesions were microdissected using an Arcturus Laser Capture microscope (Life Technologies). 12-μm cerebellum cryosections were collected on Super Frost slides (Fisher). After dehydrating the tissue, the areas of interest were captured on CapSure High Sensitivity (HS) caps using the infrared laser. DNA was isolated from the lesions using a DNA Pico Pure Isolation kit (Life Technologies).

Assessment of the Status of the *Ptch1* Wild-Type Allele

We performed qPCR on total genomic DNA isolated using a DNeasy Kit (QIAGEN). The levels of the wild-type allele of *Ptch1* relative to *Dot1l* were normalized to the IGL (for preneoplasia; Figure 3) or to the cortex (for advanced medulloblastoma; Figure 2) of *Ptch1* mice (one copy of *Ptch1*) and were obtained using the delta-delta-CT method and Sybrgreen reagents on a Viia 7 system (Life Technologies); reactions were carried in triplicate, and the amount of gDNA per reaction was 20 ng. We designed primers recognizing *Ptch*1 Exon1-Intron1-2. Since this region is deleted in the *Ptch1* mutant allele (Goodrich et al., 1997), these primers are specific for the wild-type allele of *Ptch1*.

SUPPLEMENTAL INFORMATION

Supplemental Information includes Supplemental Experimental Procedures, two figures, and one table and can be found with this article online at http://dx.doi.org/10.1016/j.celrep.2016.02.061.

AUTHOR CONTRIBUTIONS

F.C. and L.T.-O. designed the study and wrote the article. N.B., C.-L.W., A.K., S.M.S., and L.T.-O. conducted the experiments. M.R., P.S., and M.D.T. performed bioinformatics analyses of human data.

ACKNOWLEDGMENTS

We thank Frédéric Mille, Nada Jabado, Daniel Durocher, Francis Rodier, Gerardo Ferbeyre, and Elliot Drobetsky for helpful advice and Patricia T. Yam for comments on the manuscript. We thank J. Barthe for animal husbandry and J. Cardin and J.-F. Michaud for technical expertise. We thank A. Dumont and O.

Neyret for help with bisulfite sequencing. We thank Tyler Jacks and the NCI Animal Repository for kindly providing the $p53^{LSL-R172H}$ mice. This work was supported by grants from the Canadian Institutes of Health Research (CIHR), the Fonds de Recherche du Québec-Santé (FRQS), and the Canada Foundation for Innovation (CFI). L.T.-O. is recipient of the Caldas fellowship (Colciencias). F.C. holds the Canada Research Chair in Developmental Neurobiology.

Received: August 3, 2015
Revised: December 28, 2015
Accepted: February 11, 2016
Published: March 17, 2016

REFERENCES

Abe, Y., Oda-Sato, E., Tobiume, K., Kawauchi, K., Taya, Y., Okamoto, K., Oren, M., and Tanaka, N. (2008). Hedgehog signaling overrides p53-mediated tumor suppression by activating Mdm2. Proc. Natl. Acad. Sci. USA *105*, 4838–4843.

Ayrault, O., Zindy, F., Rehg, J., Sherr, C.J., and Roussel, M.F. (2009). Two tumor suppressors, p27Kip1 and patched-1, collaborate to prevent medulloblastoma. Mol. Cancer Res. *7*, 33–40.

Barnes, E.A., Kong, M., Ollendorff, V., and Donoghue, D.J. (2001). Patched1 interacts with cyclin B1 to regulate cell cycle progression. EMBO J. *20*, 2214–2223.

Braig, M., Lee, S., Loddenkemper, C., Rudolph, C., Peters, A.H., Schlegelberger, B., Stein, H., Dörken, B., Jenuwein, T., and Schmitt, C.A. (2005). Oncogene-induced senescence as an initial barrier in lymphoma development. Nature *436*, 660–665.

Carnero, A., Hudson, J.D., Price, C.M., and Beach, D.H. (2000). p16INK4A and p19ARF act in overlapping pathways in cellular immortalization. Nat. Cell Biol. *2*, 148–155.

Castellino, R.C., De Bortoli, M., Lu, X., Moon, S.H., Nguyen, T.A., Shepard, M.A., Rao, P.H., Donehower, L.A., and Kim, J.Y. (2008). Medulloblastomas overexpress the p53-inactivating oncogene WIP1/PPM1D. J. Neurooncol. *86*, 245–256.

Chen, Z., Trotman, L.C., Shaffer, D., Lin, H.K., Dotan, Z.A., Niki, M., Koutcher, J.A., Scher, H.I., Ludwig, T., Gerald, W., et al. (2005). Crucial role of p53-dependent cellular senescence in suppression of Pten-deficient tumorigenesis. Nature *436*, 725–730.

Doucette, T.A., Yang, Y., Pedone, C., Kim, J.Y., Dubuc, A., Northcott, P.D., Taylor, M.D., Fults, D.W., and Rao, G. (2012). WIP1 enhances tumor formation in a sonic hedgehog-dependent model of medulloblastoma. Neurosurgery *70*, 1003–1010, discussion 1010.

Fearon, E.R., and Vogelstein, B. (1990). A genetic model for colorectal tumorigenesis. Cell *61*, 759–767.

Frappart, P.O., Lee, Y., Russell, H.R., Chalhoub, N., Wang, Y.D., Orii, K.E., Zhao, J., Kondo, N., Baker, S.J., and McKinnon, P.J. (2009). Recurrent genomic alterations characterize medulloblastoma arising from DNA double-strand break repair deficiency. Proc. Natl. Acad. Sci. USA *106*, 1880–1885.

Gailani, M.R., Leffell, D.J., Ziegler, A., Gross, E.G., Brash, D.E., and Bale, A.E. (1996). Relationship between sunlight exposure and a key genetic alteration in basal cell carcinoma. J. Natl. Cancer Inst. *88*, 349–354.

Genovesi, L.A., Ng, C.G., Davis, M.J., Remke, M., Taylor, M.D., Adams, D.J., Rust, A.G., Ward, J.M., Ban, K.H., Jenkins, N.A., et al. (2013). Sleeping Beauty mutagenesis in a mouse medulloblastoma model defines networks that discriminate between human molecular subgroups. Proc. Natl. Acad. Sci. USA *110*, E4325–E4334.

Goodrich, L.V., Milenković, L., Higgins, K.M., and Scott, M.P. (1997). Altered neural cell fates and medulloblastoma in mouse patched mutants. Science *277*, 1109–1113.

He, X., Zhang, L., Chen, Y., Remke, M., Shih, D., Lu, F., Wang, H., Deng, Y., Yu, Y., Xia, Y., et al. (2014). The G protein α subunit Gαs is a tumor suppressor in Sonic hedgehog-driven medulloblastoma. Nat. Med. *20*, 1035–1042.

Hill, R.M., Kuijper, S., Lindsey, J.C., Petrie, K., Schwalbe, E.C., Barker, K., Boult, J.K., Williamson, D., Ahmad, Z., Hallsworth, A., et al. (2015). Combined MYC and P53 defects emerge at medulloblastoma relapse and define rapidly progressive, therapeutically targetable disease. Cancer Cell *27*, 72–84.

Hovestadt, V., Jones, D.T., Picelli, S., Wang, W., Kool, M., Northcott, P.A., Sultan, M., Stachurski, K., Ryzhova, M., Warnatz, H.J., et al. (2014). Decoding the regulatory landscape of medulloblastoma using DNA methylation sequencing. Nature *510*, 537–541.

Izzi, L., Lévesque, M., Morin, S., Laniel, D., Wilkes, B.C., Mille, F., Krauss, R.S., McMahon, A.P., Allen, B.L., and Charron, F. (2011). Boc and Gas1 each form distinct Shh receptor complexes with Ptch1 and are required for Shh-mediated cell proliferation. Dev. Cell *20*, 788–801.

Kato, S., Han, S.Y., Liu, W., Otsuka, K., Shibata, H., Kanamaru, R., and Ishioka, C. (2003). Understanding the function-structure and function-mutation relationships of p53 tumor suppressor protein by high-resolution missense mutation analysis. Proc. Natl. Acad. Sci. USA *100*, 8424–8429.

Kawauchi, D., Robinson, G., Uziel, T., Gibson, P., Rehg, J., Gao, C., Finkelstein, D., Qu, C., Pounds, S., Ellison, D.W., et al. (2012). A mouse model of the most aggressive subgroup of human medulloblastoma. Cancer Cell *21*, 168–180.

Kessler, J.D., Hasegawa, H., Brun, S.N., Emmenegger, B.A., Yang, Z.J., Dutton, J.W., Wang, F., and Wechsler-Reya, R.J. (2009). N-myc alters the fate of preneoplastic cells in a mouse model of medulloblastoma. Genes Dev. *23*, 157–170.

Kool, M., Jones, D.T., Jäger, N., Northcott, P.A., Pugh, T.J., Hovestadt, V., Piro, R.M., Esparza, L.A., Markant, S.L., Remke, M., et al.; ICGC PedBrain Tumor Project (2014). Genome sequencing of SHH medulloblastoma predicts genotype-related response to smoothened inhibition. Cancer Cell *25*, 393–405.

Ling, G., Ahmadian, A., Persson, A., Undén, A.B., Afink, G., Williams, C., Uhlén, M., Toftgård, R., Lundeberg, J., and Pontén, F. (2001). PATCHED and p53 gene alterations in sporadic and hereditary basal cell cancer. Oncogene *20*, 7770–7778.

Malek, R., Matta, J., Taylor, N., Perry, M.E., and Mendrysa, S.M. (2011). The p53 inhibitor MDM2 facilitates Sonic Hedgehog-mediated tumorigenesis and influences cerebellar foliation. PLoS ONE *6*, e17884.

Michaloglou, C., Vredeveld, L.C., Soengas, M.S., Denoyelle, C., Kuilman, T., van der Horst, C.M., Majoor, D.M., Shay, J.W., Mooi, W.J., and Peeper, D.S. (2005). BRAFE600-associated senescence-like cell cycle arrest of human naevi. Nature *436*, 720–724.

Mille, F., Thibert, C., Fombonne, J., Rama, N., Guix, C., Hayashi, H., Corset, V., Reed, J.C., and Mehlen, P. (2009). The Patched dependence receptor triggers apoptosis through a DRAL-caspase-9 complex. Nat. Cell Biol. *11*, 739–746.

Mille, F., Tamayo-Orrego, L., Lévesque, M., Remke, M., Korshunov, A., Cardin, J., Bouchard, N., Izzi, L., Kool, M., Northcott, P.A., et al. (2014). The Shh receptor Boc promotes progression of early medulloblastoma to advanced tumors. Dev. Cell *31*, 34–47.

Narita, M., and Lowe, S.W. (2005). Senescence comes of age. Nat. Med. *11*, 920–922.

Olive, K.P., Tuveson, D.A., Ruhe, Z.C., Yin, B., Willis, N.A., Bronson, R.T., Crowley, D., and Jacks, T. (2004). Mutant p53 gain of function in two mouse models of Li-Fraumeni syndrome. Cell *119*, 847–860.

Oliver, T.G., Read, T.A., Kessler, J.D., Mehmeti, A., Wells, J.F., Huynh, T.T., Lin, S.M., and Wechsler-Reya, R.J. (2005). Loss of patched and disruption of granule cell development in a pre-neoplastic stage of medulloblastoma. Development *132*, 2425–2439.

Pazzaglia, S., Tanori, M., Mancuso, M., Gessi, M., Pasquali, E., Leonardi, S., Oliva, M.A., Rebessi, S., Di Majo, V., Covelli, V., et al. (2006). Two-hit model for progression of medulloblastoma preneoplasia in Patched heterozygous mice. Oncogene *25*, 5575–5580.

Pei, Y., Moore, C.E., Wang, J., Tewari, A.K., Eroshkin, A., Cho, Y.J., Witt, H., Korshunov, A., Read, T.A., Sun, J.L., et al. (2012). An animal model of MYC-driven medulloblastoma. Cancer Cell *21*, 155–167.

Pugh, T.J., Weeraratne, S.D., Archer, T.C., Pomeranz Krummel, D.A., Auclair, D., Bochicchio, J., Carneiro, M.O., Carter, S.L., Cibulskis, K., Erlich, R.L., et al. (2012). Medulloblastoma exome sequencing uncovers subtype-specific somatic mutations. Nature *488*, 106–110.

Quelle, D.E., Cheng, M., Ashmun, R.A., and Sherr, C.J. (1997). Cancer-associated mutations at the INK4a locus cancel cell cycle arrest by p16INK4a but not by the alternative reading frame protein p19ARF. Proc. Natl. Acad. Sci. USA *94*, 669–673.

Rausch, T., Jones, D.T., Zapatka, M., Stütz, A.M., Zichner, T., Weischenfeldt, J., Jäger, N., Remke, M., Shih, D., Northcott, P.A., et al. (2012). Genome sequencing of pediatric medulloblastoma links catastrophic DNA rearrangements with TP53 mutations. Cell *148*, 59–71.

Robinson, G., Parker, M., Kranenburg, T.A., Lu, C., Chen, X., Ding, L., Phoenix, T.N., Hedlund, E., Wei, L., Zhu, X., et al. (2012). Novel mutations target distinct subgroups of medulloblastoma. Nature *488*, 43–48.

Stecca, B., and Ruiz i Altaba, A. (2009). A GLI1-p53 inhibitory loop controls neural stem cell and tumour cell numbers. EMBO J. *28*, 663–676.

Taylor, M.D., Northcott, P.A., Korshunov, A., Remke, M., Cho, Y.J., Clifford, S.C., Eberhart, C.G., Parsons, D.W., Rutkowski, S., Gajjar, A., et al. (2012). Molecular subgroups of medulloblastoma: the current consensus. Acta Neuropathol. *123*, 465–472.

Thomas, W.D., Chen, J., Gao, Y.R., Cheung, B., Koach, J., Sekyere, E., Norris, M.D., Haber, M., Ellis, T., Wainwright, B., and Marshall, G.M. (2009). Patched1 deletion increases N-Myc protein stability as a mechanism of medulloblastoma initiation and progression. Oncogene *28*, 1605–1615.

Uziel, T., Zindy, F., Xie, S., Lee, Y., Forget, A., Magdaleno, S., Rehg, J.E., Calabrese, C., Solecki, D., Eberhart, C.G., et al. (2005). The tumor suppressors Ink4c and p53 collaborate independently with Patched to suppress medulloblastoma formation. Genes Dev. *19*, 2656–2667.

Ventura, A., Kirsch, D.G., McLaughlin, M.E., Tuveson, D.A., Grimm, J., Lintault, L., Newman, J., Reczek, E.E., Weissleder, R., and Jacks, T. (2007). Restoration of p53 function leads to tumour regression in vivo. Nature *445*, 661–665.

Wetmore, C., Eberhart, D.E., and Curran, T. (2001). Loss of p53 but not ARF accelerates medulloblastoma in mice heterozygous for patched. Cancer Res. *61*, 513–516.

Zhang, H., Ping, X.L., Lee, P.K., Wu, X.L., Yao, Y.J., Zhang, M.J., Silvers, D.N., Ratner, D., Malhotra, R., Peacocke, M., and Tsou, H.C. (2001). Role of PTCH and p53 genes in early-onset basal cell carcinoma. Am. J. Pathol. *158*, 381–385.

Zhukova, N., Ramaswamy, V., Remke, M., Pfaff, E., Shih, D.J., Martin, D.C., Castelo-Branco, P., Baskin, B., Ray, P.N., Bouffet, E., et al. (2013). Subgroup-specific prognostic implications of TP53 mutation in medulloblastoma. J. Clin. Oncol. *31*, 2927–2935.